DRP-1-14
April 1994

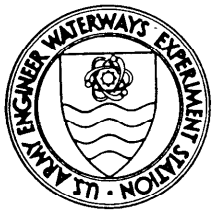

Dredging Research Technical Notes

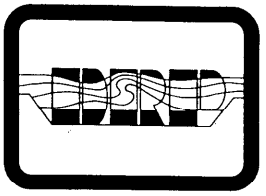

Water Wave Attenuation Over Nearshore Underwater Mudbanks and Mud Berms

Purpose

A shallow-water wave-mud interaction model is described and used to discuss design parameters for berms constructed from fine-grained sediment. Model application is presented to determine the stable elevation of the berm crest and the water column height above the crest in a given coastal environment. The model will predict wave attenuation and considers water to be inviscid and mud to be a highly viscous fluid. It is the simplest model applicable.

Background

Naturally occurring underwater mudbanks are known to absorb water wave energy and thereby attenuate waves that pass over them. Energy reductions on the order of 30 percent to as much as 90 percent are common even in the absence of any measurable wave breaking. In recent years, engineering efforts have made use of this property by creating underwater mud berms to lessen wave impact in the area leeward of the berm. Thus, by appropriately placing fine-grained dredged material from navigation channels, the disposed material can be made to serve beneficially.

The capacity of naturally occurring bottom mud to absorb wave energy in coastal areas has been known for years, and in recent times this property has been recognized as a potential means for protecting beaches that are susceptible to erosion under wave attack. As an example of the former, prominent mudbanks occur on the eastern margin of the Louisiana chenier plain where episodic waves are measurably damped as they pass shoreward over the banks. The alongshore length of the banks varies from 1 to 5 km, width from 0.5 to 3 km, and thickness from 0.2 to 1.5 m, in water depths from 1 to 2 m above the mud surface. The median particle size is 3 to 5 μm (Wells 1983, Wells and Kemp 1986).

As an example of a nonsacrificial, engineered berm off Dauphin Island in Alabama, an underwater mound composed of sediment dredged from

US Army Engineer Waterways Experiment Station
3909 Halls Ferry Road, Vicksburg, MS 39180-6199

the Mobile Ship Channel within Mobile Bay was deposited by the U.S. Army Engineer District, Mobile, in 1988. The design dimensions of the berm were 2,750 m alongshore, 300 m wide at the toe, and 6 m high with 6.5 m mean depth of water above the berm crest (McLellan, Pope, and Burke 1990). The placed material is highly graded, with a median size of about 15 μm.

The degree to which such natural or manmade coastal features attenuate incoming wave energy depends on their dimensions, the composition of the sediment, and the incoming wave characteristics. Thus, a predictive method for berm design must include the essential physical modes of interaction between the flow and the dissipative bottom material. The two most important berm design parameters are the crest elevation and the depth of water above the crest, since these measurably influence the degree of wave attenuation, and hence, the wave impact in sheltered areas.

Research performed under the Dredging Research Program (DRP) Technical Area 1, Work Unit "Cohesive Sediment Processes," has included laboratory tests on wave damping and fluidization of mud, and the development of two wave-mud interaction models. The first and simplest model assumes the mud to be a viscous fluid and the shallow-water waves to be linear, while the second model considers the mud to be viscoelastic and the waves to be finite amplitude (nonlinear). The simple model is used in this technical note as a guide for berm design and to demonstrate the general approach.

Additional Information

This technical note is based on work by Drs. Ashish Mehta and Feng Jiang at the University of Florida under contract to the DRP. For additional information, contact Mr. Allen Teeter, (601) 634-2820, or the DRP manager, Mr. E. Clark McNair, (601) 634-2070.

General Physical Setting and Processes

The physical setting relative to the mudbank or the underwater berm is conceptually shown in Figure 1. Seawater (density ρ, dynamic viscosity μ) surrounds the mud berm, which is in general a viscoelastic material (density ρ_M) possessing both an elastic component characterized by the shear modulus G (typically on the order of 10^1 to 10^4 Pa) and viscosity μ_M (typically on the order of 10^1 to 10^4 Pa · sec). (A notation list is provided as Table 1.) Most muds are pseudoplastics in terms of the relation between the shear stress and the rate of strain, so that they exhibit creep even at very low applied stresses. *Dredging Research Technical Notes* DRP-2-04 (Teeter 1992) describes the general aspects of channel-bottom mud viscous characteristics.

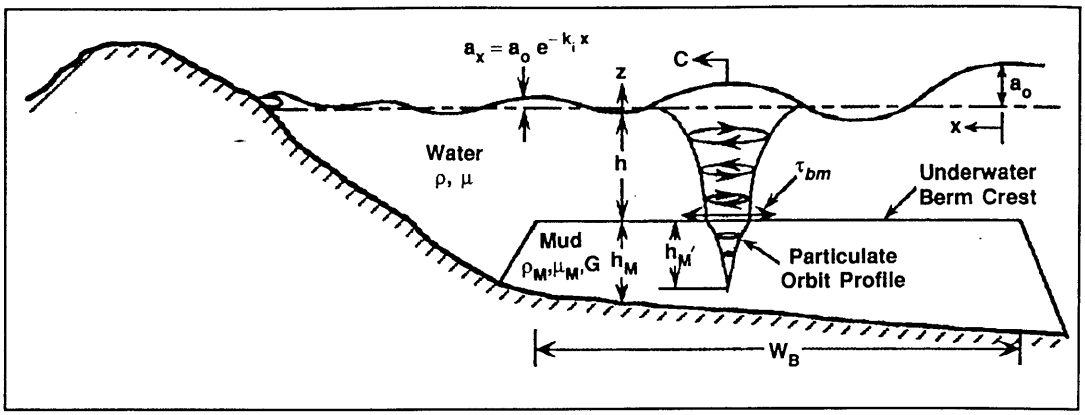

Figure 1. Schematic sketch showing wave propagation over an underwater mud berm

When subjected to wave action, bottom muds respond by oscillating at the forcing wave frequency. As a result of high viscosity, the oscillations attenuate much more rapidly with depth within mud than in the water column above. A high rate of energy dissipation within the mud causes the surface wave height to decrease rapidly with onshore distance. Thus, given the surface wave amplitude a_0 at $x = 0$ at the seaward edge of the berm crest, the amplitude at any distance x, that is, $a_x = a_0 \exp(-k_i x)$, depends on the wave attenuation coefficient k_i. If the bottom were rigid, k_i would be on the order of 10^{-5} m^{-1}, whereas for mud, values as high as 10^{-4} to 10^{-3} m^{-1} are common (Jiang and Mehta 1992). The effect is much reduced wave activity in the area leeward of a mud berm compared with areas where the bottom is composed of hard material. On the other hand, the wave celerity is higher where mud is the substrate because the available depth for wave propagation is effectively greater than the water depth, h. Consequently, the depth h_M, shown in Figure 1, requires specification.

Mud oscillation primarily occurs as a result of wave-induced pressure work within the body of the material, while the effect of shear stress is more important at the mud surface where it can cause particulate resuspension. Thus, under continued wave action, the long-term equilibrium water depth above the crest is that depth at which the wave-induced hydraulic shear stress amplitude τ_{bm} is equal to the erosion shear strength τ_s of mud.

In many naturally occurring environments, mud oscillations under typical fair-weather wave conditions occur without much sediment resuspension and associated turbidity (Jiang and Mehta 1992). Thus, $\tau_{bm} = \tau_s$ can be used as a design criterion for the berm crest elevation and the berm can fulfill its role as a wave attenuator without generating excessive turbidity and dispersion from the site through transport of eroded sediment.

The berm slope from crest to toe is determined by a characteristic yield strength, which for design purposes has been approximated by the upper-Bingham yield strength τ_y of the pseudoplastic material (Migniot 1968).

Table 1. Notation Definitions	
Notation	**Definition**
a_0	Surface wave amplitude at the offshore berm toe ($x = 0$), m
a_x	Surface wave amplitude at some inshore distance x, m
g	Acceleration of gravity, m/sec^2
G	Shear modulus, Pa
h	Water depth, m
h_M	Mud depth or thickness, m
h_M'	Wave boundary layer thickness in mud, m
k	Wave number, m^{-1}
k_i	Wave attenuation coefficient, m^{-1}
t	Starting time, day
t_e	Equilibrium time, days
u	Wave-induced water velocity, m/sec
u_L	Wave-induced Stokes' drift in mud, m/sec
u_M	Wave-induced mud velocity, m/sec
x	Distance inshore of offshore berm toe, m
α	Friction coefficient, Pa · sec^2/m^2
α'	Slope angle, deg
β	Empirical slope constant, deg/Pa
γ	Normalized density jump $(\rho_M - \rho)/\rho_M$
ζ	Nondimensional wave number
η	Water surface deviation, m
η_M	Mud surface deviation, m
μ	Dynamic viscosity of water, Pa · sec
μ_M	Dynamic viscosity of mud, Pa · sec
ν_M	Kinematic viscosity, m^2/sec
ξ	Nondimensional wave attenuation coefficient
ρ	Water density, kg/m^3
ρ_M	Mud density, kg/m^3
σ	Wave angular frequency, rad/sec
τ_{bm}	Hydraulic shear stress at mud surface, Pa
τ_s	Erosion threshold for mud, Pa
τ_y	Upper-Bingham yield stress, Pa
χ	Nondimensional mud depth

However, the stability of the berm crest is not ensured solely through this criterion for erosion since, due to open particle orbits (Figure 2) arising from nonlinear wave effects, the residual velocity u_L (Stokes' drift) can cause the mud mass to be transported landward. The impetus for this motion is the net wave-induced thrust that occurs in the mud due to the rapid wave attenuation with onshore distance. Thus, hypothetically starting at time t with a mud-water interfacial profile that can be shown to be near-exponential in form (Jiang 1993), the depth-averaged value of u_L will become nil everywhere at some instant t_e, when an equilibrium interfacial profile is established. Such a condition will result from a balance between the wave-induced thrust and the adverse hydrostatic gradient in the presence of a sloping bottom, as shown in Figure 2. Profiles such as these are seasonally established, for instance, along the southwest coast of India off Kerala, where the southwesterly monsoon waves push the mudbanks from about 20-m water depth to a position close to the shoreline.

Figure 3 shows the region offshore of the town of Alleppey in Kerala where wave spectra were obtained at two sites (Mathew 1992). The mean depth of water at the offshore site was 10 m, and at the inshore site a little over 5 m. In fair weather, the mudbank off Kerala stays well seaward of the offshore site.

Figure 4 is a schematic profile of the Kerala mudbank at its nearshore location (Nair 1988). Its position has been stabilized against the comparatively steep nearshore bottom. During two particular monsoon periods, the shoreward edge of the mudbank was landward of the inshore measurement site, while the seaward edge of the mudbank was landward of the offshore measurement site. Thus, the bottom at the offshore site was consistently devoid of mud. Figure 5 shows examples of wave spectra, with and without the mudbank present, at the inshore site. In fair weather, the energy reduction was negligible. (Note the slight phase shift of the inshore spectrum relative to offshore, which may be an artifact of the data analysis. If a physical basis was the cause, it remains unidentified.)

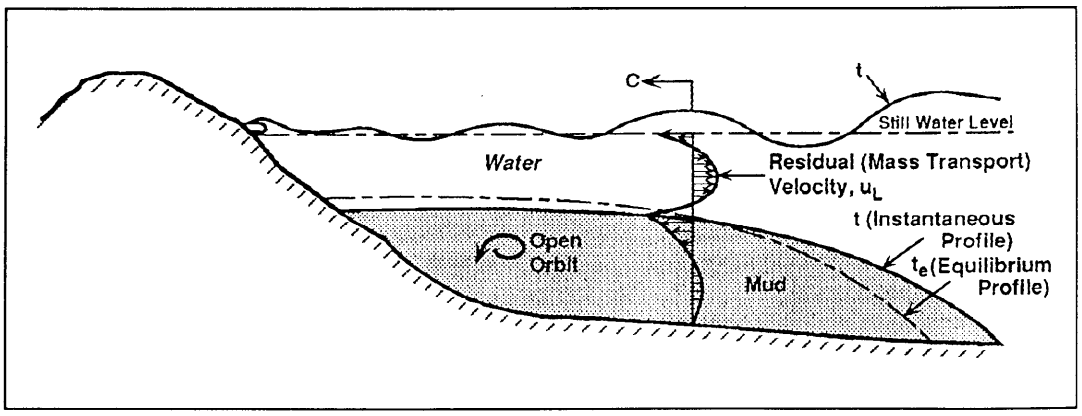

Figure 2. Elevation sketch showing mudbank and its motion due to Stokes' drift

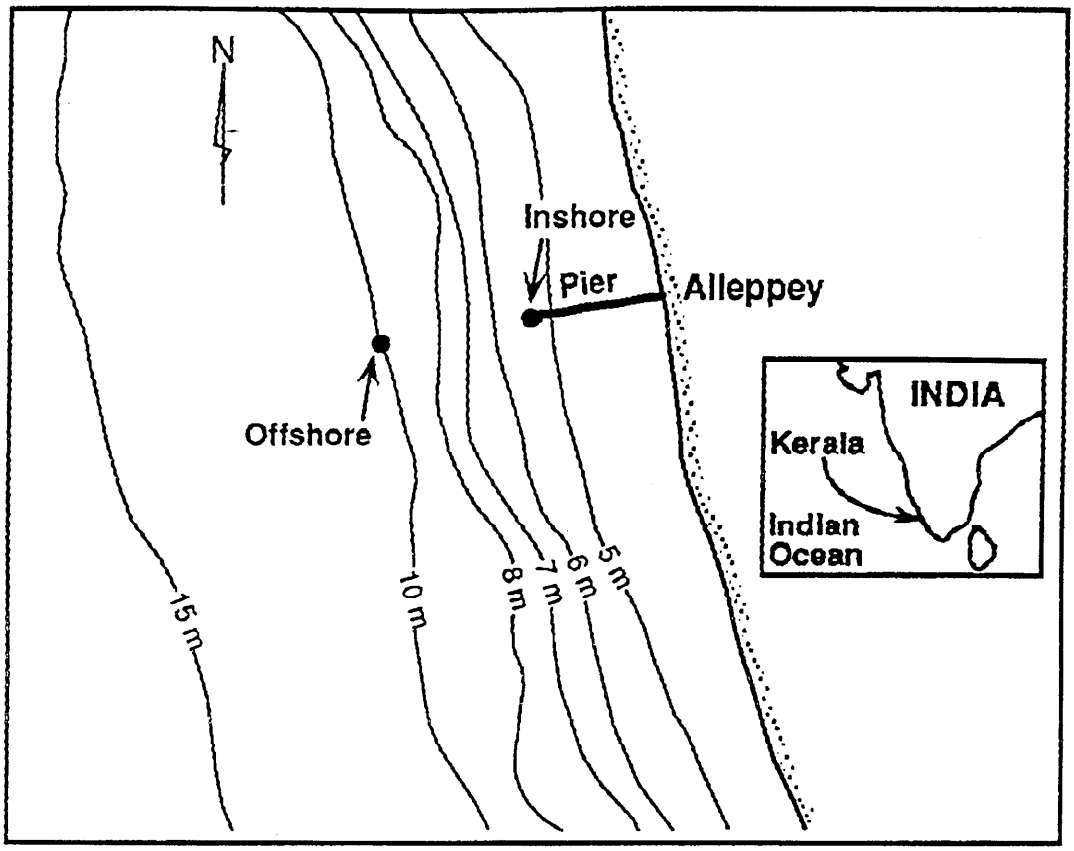

Figure 3. Coastal site at Alleppey in Kerala, India, where monsoonal, shore-parallel mudbanks occur. The pier is 300 m long (after Mathew 1992)

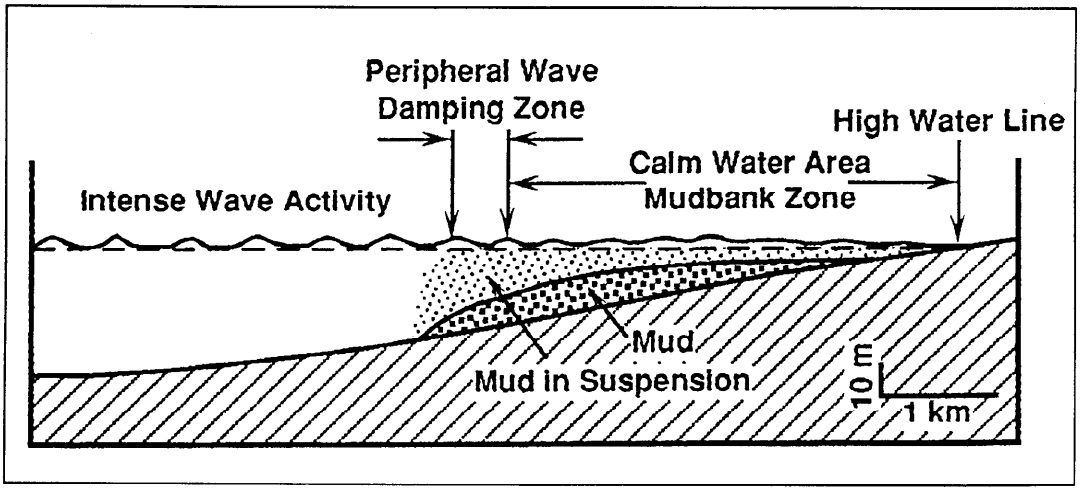

Figure 4. Schematic profile of mudbank region off the coast of Kerala, India (after Nair 1988)

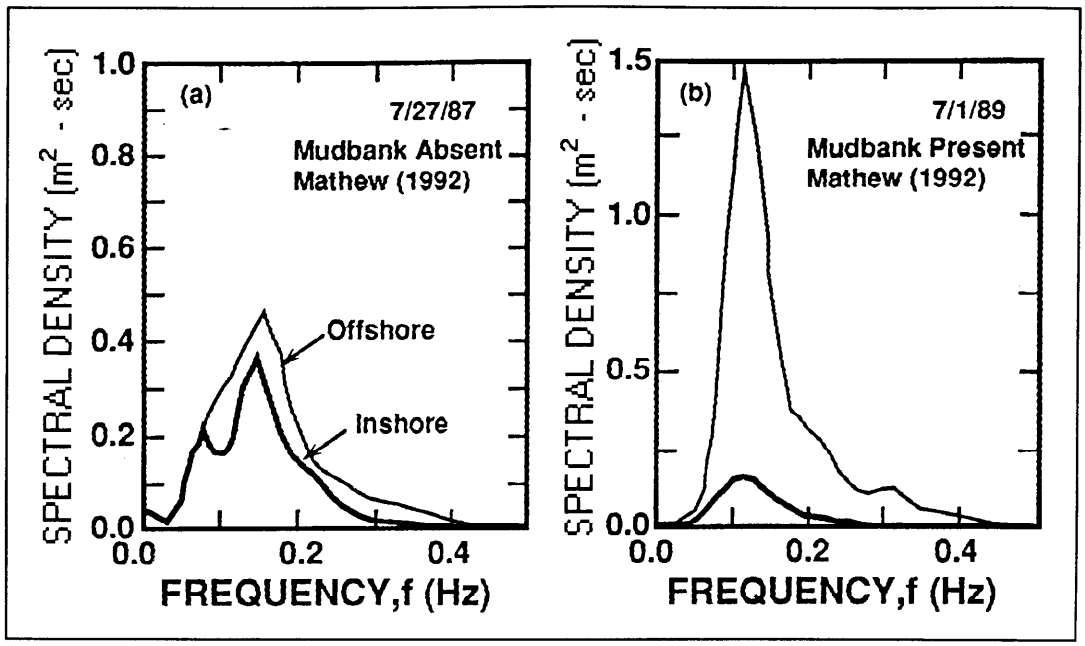

Figure 5. Offshore and inshore wave spectra off Alleppey: (a) without mudbank, and (b) with mudbank present (after Mathew 1992)

In the monsoon case, the wave energy reduction was about 85 percent at the inshore site. In fact, as a result of the mudbank, the wave energy at the inshore site was lower in monsoon than in fair weather, despite the occurrence of considerably more inclement offshore wave activity during the monsoon. Not surprisingly, during monsoon the mudbanks in Kerala have served as safe, open-coast havens for small fishing boats that would otherwise require sheltered harbors (Nair 1988).

The site of the Mobile berm, in a somewhat idealized configuration, is shown in Figure 6. Examples of offshore/inshore wave spectra are given in Figure 7 under two offshore wave conditions. Wave energy reductions were significant, 29 and 46 percent, respectively, although not nearly as dramatic as at Kerala because the finer and more clayey Kerala mud is more dissipative. Also, the Mobile berm is quite narrow compared with the mudbank. Using a hydrodynamic wave model, McLellan, Pope, and Burke (1990) showed that an assumed rigid berm crest

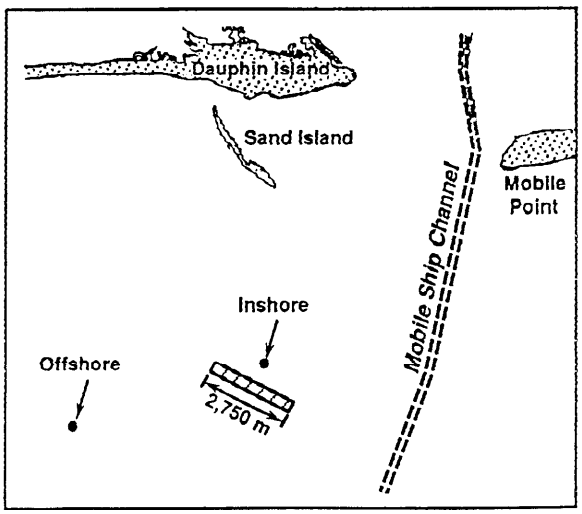

Figure 6. Construction site (corridor for dredged material placement) for the Mobile berm (after McLellan, Pope, and Burke 1990)

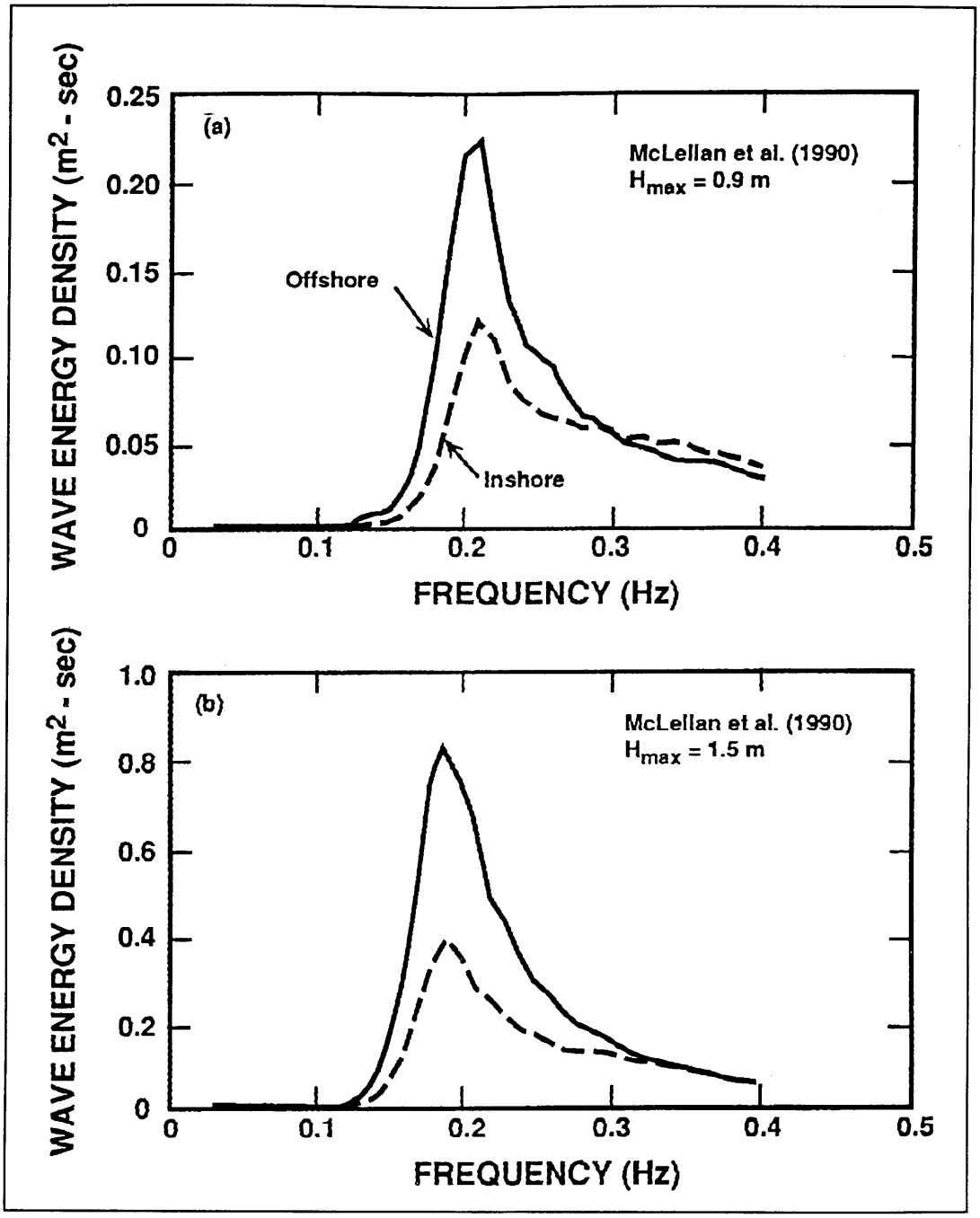

Figure 7. Offshore and inshore wave spectra at the Mobile berm site for two different wave conditions at the offshore site characterized by the maximum wave height, H_{max}: (a) H_{max} = 0.9 m, and (b) H_{max} = 1.5 m (after McLellan, Pope, and Burke 1990)

produced negligible wave energy dissipation. It is believed that as a result of the depth of water, on the order of 6.5 m over the berm, the main cause of the observed damping is energy absorption by the deposited mud at the berm site.

Interestingly, diver observations at the Mobile berm site have suggested the occurrence of surface wave-forced interfacial mud waves propagating along the compliant crest. Such bed movement confirms the participation of the bottom material in the energy dissipation process. Furthermore, the observed stability of the berm points to the fact that wave action becomes sufficiently weak over the berm to prevent significant wave-induced scour and degradation of the berm.

Mass transport due to Stokes' drift is important in situations such as those described earlier for Kerala during the Indian monsoon when sustained and significant wave action may occur for periods of weeks or months. Furthermore, the occurrence of a gravity slide into deeper waters at the cessation of high wave action toward the end of the monsoon causes the situation to be reinitialized with respect to mass transport at onset of the following monsoon. Field evidence elsewhere, for example off Surinam (Wells 1983), indicates that unlike the Kerala mudbanks that are clearly quite transitory, mudbanks typically tend to remain practically stationary because of small bottom slopes, mild and/or constant wave action, or other conditions. Consequently, their net motion need not be considered in simple calculations for stable berm design.

A Simplified Approach to Berm Design

Consideration is given to the berm elevation and water depth. It is assumed that the berm is endless in the longshore direction. This assumption requires the berm to be much longer than the length of the wave. End effects are therefore ignored alongshore, but seaward edge effects can be prominent in the cross-shore direction if the side slope is steep and the crest elevation high enough to cause an abrupt depth change at the seaward edge. Furthermore, a change in the sediment composition between the ambient bottom and the berm may also measurably influence the wave field. The mechanics of propagation of the wave over the berm would thus become an initial (spatial) value problem, the initial wave amplitude a_0 condition being defined at the toe of the berm. For typical natural mudbanks, the crest elevations are not high and side slopes are mild. The only real change encountered sometimes is the bottom composition. Even at berms constructed by dredged material placement, side slopes are not always very steep; at the Mobile site, the slopes range from 1:24 to 1:130. Thus, for simplicity, the effects of both changing depth and bottom composition on the dissipation process over the berm can be assumed to be negligible.

Harmonic solutions involving wave propagation in a single x direction in water of depth h, over mud of thickness h_M (= h_M'), as shown in Figure 1, were found for the wave speed and other wave-induced quantities. The rheological constitutive properties of mud are important, and various viscoelastic models have been considered (such as Chou 1989 and Jiang 1993). Recent studies on wave-mud interaction by Feng et al. (1992) suggest that wave pressure work can cause the otherwise undisturbed mud

to weaken through thixotropic yield, leading to plastic behavior and loss of effective stress. This process of fluidization is reflected in a drastic reduction in the shear modulus G, with the result that the weakened mud can be approximated as a highly viscous fluid. In this technical note, for simplicity, mud is assumed to be a viscous fluid and water is inviscid. The shallow-water assumption is invoked, and the wave propagation problem is considered to be linear. These two assumptions have been relaxed in Jiang (1993) to account for the effects of finite amplitude (nonlinear) waves in intermediate water depths.

As a result of the shallow-water assumption, only horizontal motion is considered in the governing equations of motion and continuity for the water layer (characterized here by no subscript) and for the mud layer (subscript M). The horizontal x and the vertical y axes are located at the rigid bottom; surface deviations $\eta(x,t)$ and $\eta_M(x,t)$ are functions of x and time t; $u(x,t)$ and $u_M(x,y,t)$ are the wave-induced velocities; γ is the normalized density jump; h_i is the elevation of the water-mud interface; and ν is the kinematic viscosity of mud. Thus, $\gamma = (\rho_M - \rho)/\rho_M$, $h_i = h_M + \eta_M$, and $\nu_M = \mu_M/\rho_M$, where μ_M is the dynamic viscosity.

Details of solutions for the shallow-water wave equations of motion and continuity for the two-layer system including η, u, η_M, and u_M are presented by Jiang (1993). The validity of the results has been demonstrated by comparison to previous laboratory experiments by Gade (1958). The results have also been applied to measurements obtained at a site in the littoral margin of Lake Okeechobee, Florida, where about one third the bottom consists of a mud layer of peaty origin (maximum thickness 0.8 m) (Jiang and Mehta 1992). Wave damping is often significant. During a field deployment it was estimated that the wave heights were about one fourth the value that would have occurred if the bottom had been rigid. Data at the shallow-water site consisted of surface wave, water velocity, and mud acceleration spectra. The water depth was 1.43 m, and mud thickness 0.55 m. Using the wave spectrum as input, the velocity and acceleration spectra were predicted and compared with field data. The model was able to reproduce important features of the velocity and acceleration spectra. However, discrepancies between measurements and simulations occurred because of limitations in the model, especially the assumption of a viscid, nonelastic mud (Jiang 1993), and possibly because of difficulties in data collection (Jiang and Mehta 1992).

The analytic solutions for the wave attenuation coefficient and the wave number are presented graphically. In Figure 8, the dimensionless wave attenuation coefficient, $\xi = k_i/[\sigma/(gh)^{1/2}]$, where g is gravitational acceleration and σ is the angular frequency of the wave, is plotted as a function of the dimensionless mud depth, $\chi = h_M(2\mu_M/\rho_M\sigma)^{1/2}$, for h_M/h ranging from 0.1 to 1. This solution is valid only for $\gamma = (\rho_M - \rho)/\rho_M = 0.15$, which is, however, a typical value. It can be shown that $(2\mu_M/\rho_M\sigma)^{1/2}$ is representative of the thickness of the wave boundary layer in mud. For a given water depth and angular wave frequency σ, attenuation is observed to be maximum for all h_M/h, when χ is equal or close to unity.

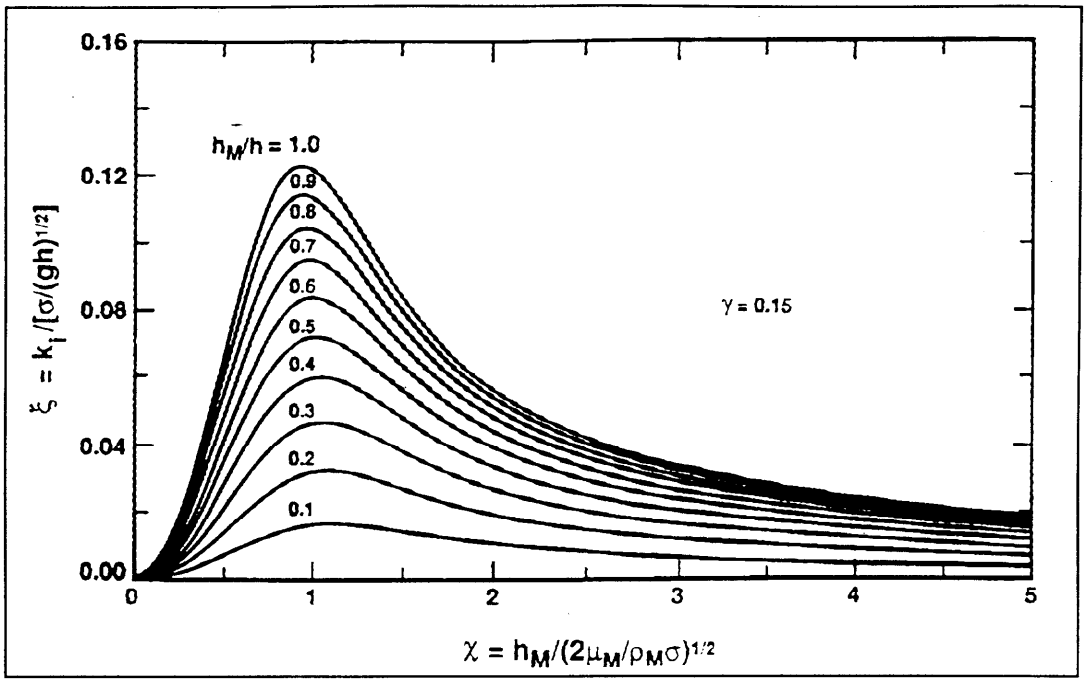

Figure 8. Relationship between ξ and χ representing the effects of wave energy dissipation in mud on wave attenuation in shallow water. (Corresponding wave number presented in Figure 9)

Therefore, this condition of maximum k_i means that the rate of wave energy dissipation in the mud is maximum when the wave boundary layer attains about the same thickness as the mud.

Two solution limits must be mentioned. One is $\chi = 0$, which corresponds to a mud of infinitely high viscosity corresponding to a rigid bottom. In this case, there is no participation by mud in the dissipation process and, since water is assumed to be inviscid, there is no damping. The other limit is approached with increasing χ corresponding to decreasing mud viscosity. In this case, damping also approaches zero as suggested by the display.

In Figure 9, the companion plot for determining the wave number k is given. The dimensionless wave number $\zeta = k/[\sigma/(gh)^{1/2}]$ is shown as a function of χ. At $\chi = 0$, $\zeta = 1$ corresponds to shallow-water wave motion in depth h, whereas with increasing χ mud depth increases, and in the limit the problem becomes one of inviscid, shallow-water wave propagation in depth $h + h_M$. Note that the solution for the maximum crest water velocity amplitude at the seaward edge of the berm crest is $u_M = a_0 g k/\sigma$. Thus, the shear stress amplitude at the mud surface is $\tau_{bm} = \alpha\, u_M^2$ where α incorporates water density and a drag term that depends on the roughness of the mud surface as well as the amplitude of the water particle just above the mud surface (Dyer 1986).

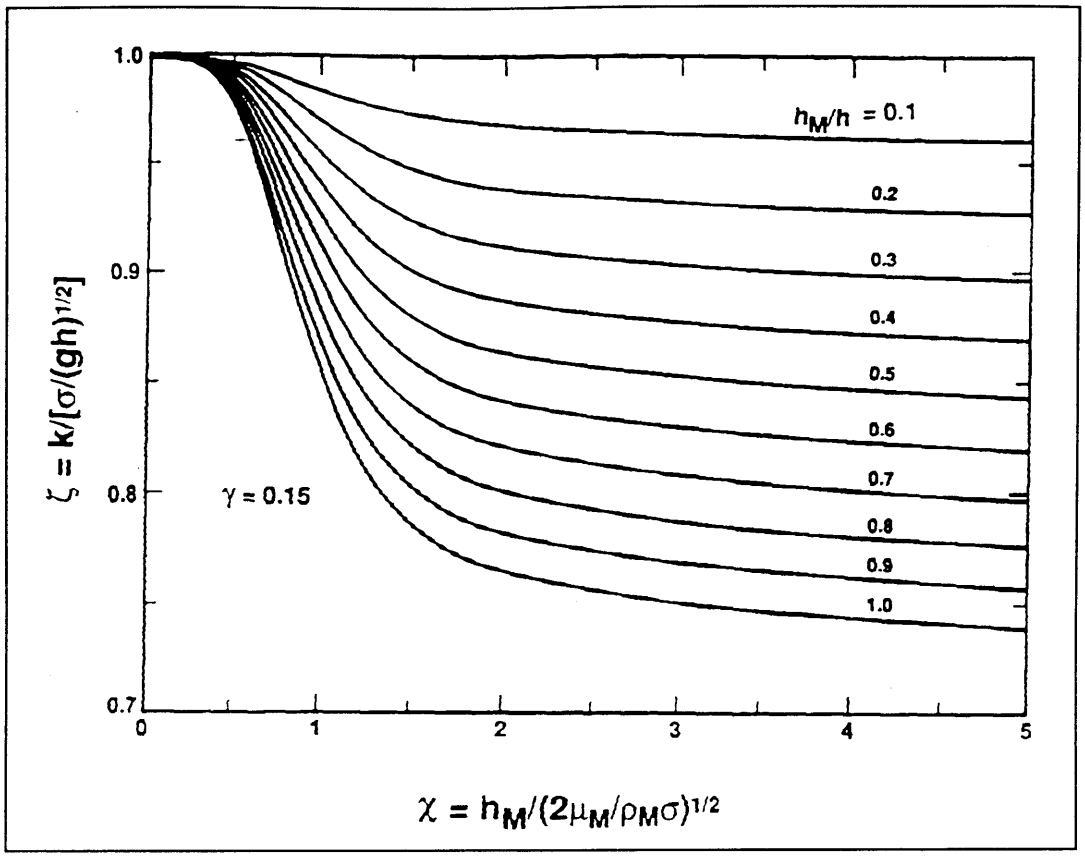

Figure 9. Relationship between ζ and χ, for determining the wave number corresponding to Figure 8

Example Application

These solutions can be used to address a simple, hypothetical berm design problem. Assume a 3-m-high ($h_M' = h_M$) fine-grained, dredged material (density 1,180 kg/m^3) mound structure in water such that it remains stable. At the same time, the economics of dredged material transport dictates that the structure be placed in the shallowest possible depth to minimize the distance between the shoreline and the structure. Other relevant parameters are wave frequency $\sigma = 0.2\pi$ rad/sec, forcing wave amplitude $a_0 = 0.75$ m, erosion shear stress $\tau_s = 1$ Pa, and $\alpha = 1.03$ Pa $\cdot$ sec^2/m^2 for a hydraulically smooth turbulent flow. First examine the effect of mud viscosity on the problem by selecting two values of the mud kinematic viscosity, $\nu_M = \mu_M/\rho_M = 10^{-3}$ and 10^{-1} m^2/sec. Then, find the water depth h and calculate wave attenuation, assuming the berm to be 300 m wide (w_B in Figure 1).

For this case the dimensionless mud depth $\chi = 53$ and 5.3 for the low- and high-viscosity values. Figures 8 and 9 can then be used to find the dependence of the wave number k, the wave attenuation coefficient k_i, and the bed shear stress amplitude at the berm crest τ_{bm} on the water depth h. In Figure 10, these relationships are shown graphically for depth h

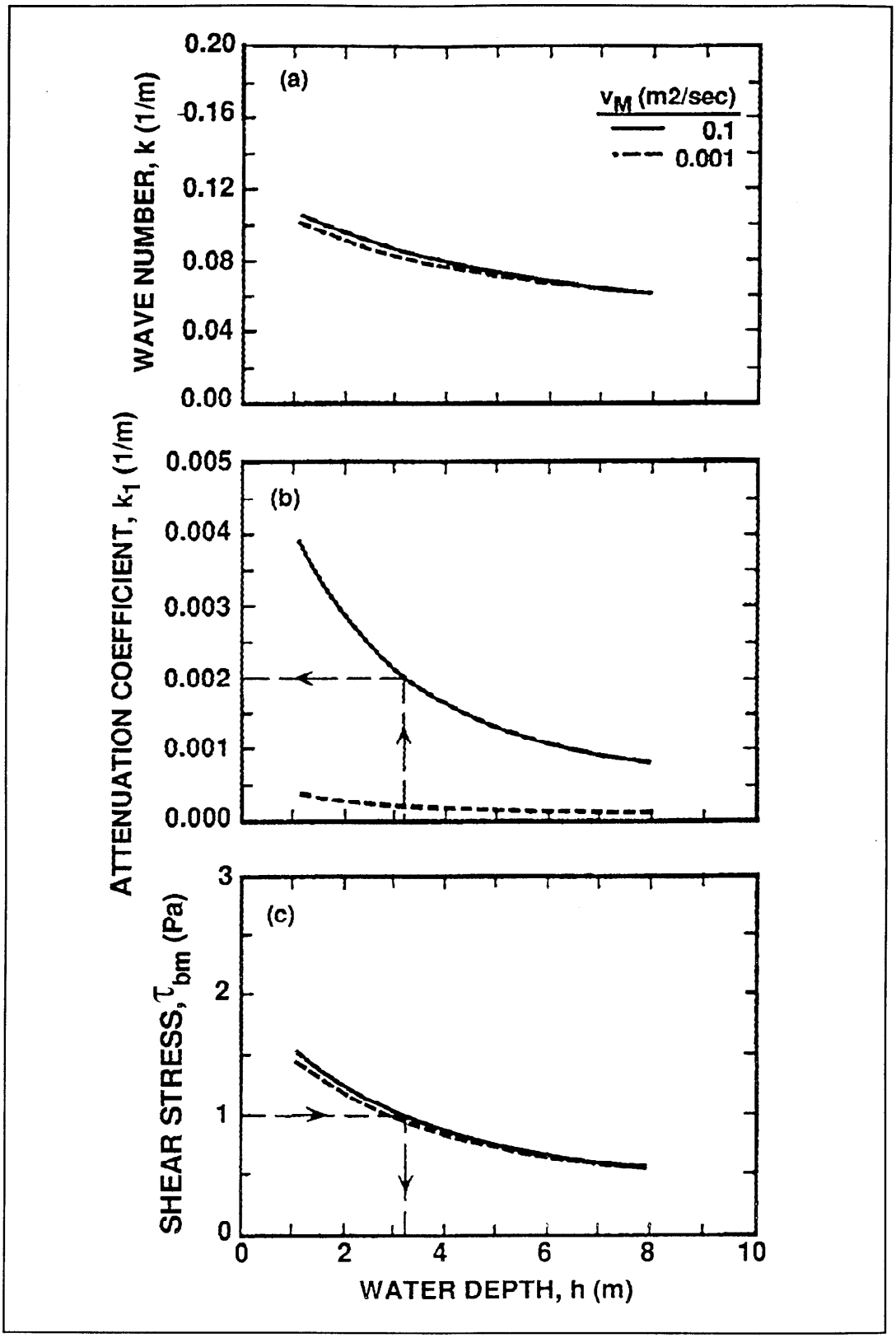

Figure 10. Effect of mud viscosity on relationships relevant to berm design: (a) wave number versus water depth, (b) wave attenuation coefficient versus water depth, and (c) bed shear stress amplitude versus water depth

ranging from 1 to 8 m. Note that for the chosen wave frequency, the model cannot be used for greater depths because of the shallow-water assumption. The wave number is seen to be comparatively insensitive to viscosity, since it depends primarily on the inertia and pressure forces in the water column. The same is observed in the case of the bed shear stress.

Note also that the magnitude of the bed shear stress is an artifact of its chosen dependence on the water velocity in the inviscid water column under the given assumptions. This dependence is characterized by the coefficient α. On the other hand, wave damping is seen to be highly sensitive to the viscosity, which emphasizes the need to appropriately consider the composition and the constitutive behavior of the particular mud under investigation.

Given the erosion shear stress τ_s = 1 Pa, the minimum water depth required for a stable berm would be 3.2 m (Figure 10c), using the higher of the two viscosities as most realistic. The site where this depth occurs will be the minimum distance from the shoreline where the berm must be placed for it to be nonsacrificial. Since for the depth of 3.2 m the wave attenuation coefficient k_i = 0.002 1/m, the 1.5-m-high wave will be reduced to 0.82 m, which corresponds to a 70-percent reduction in the wave energy.

Information on the berm crest elevation and the minimum water depth for a stable berm must be supplemented by other design parameters for engineering implementation of berm design. Among these, berm slope is perhaps most important. In that context the relationship of Migniot (1968), $\tan \alpha' = \beta\tau_y$, where α' is the slope (angle), is worth a note. From laboratory experiments the empirical constant β was found to vary from 0.007 to 0.025 when the yield stress τ_y was measured in pascals. If for the sake of argument it is assumed that $\tau_y = \tau_s$ = 1 Pa, the corresponding range of slope will be 1:143 to 1:40, which is realistic when compared with 1:130 to 1:24 at the Mobile berm.

Conclusions

The Mobile berm appears to be effective in damping approaching water waves because of the highly dissipative nature of the mud bottom. In that context, the model presented here is a useful tool for examining the essential physics underlying the dissipative mechanism, which is almost entirely embodied in the rheology of the mud. An application of the shallow-water model to calculate design berm crest elevation and water depth was presented. The model relies on a minimum of input information and is amenable to graphical presentation of berm design calculations. In some cases, however, the more complex model presented by Jiang (1993) may be more appropriate. It better incorporates physics of the wave-mud interaction problem, and can be potentially used for berm design calculations under conditions for which the assumptions

underlying the shallow-water model are not valid. That model can also be used to assess potential wave impacts where a preexisting berm or a bank is removed naturally or otherwise, thus exposing a hard bottom over which wave dissipation would be reduced.

References

Chou, H. T. 1989. "Rheological Response of Cohesive Sediments to Water Waves," Ph.D. dissertation, University of California, Berkeley.

Dyer, K. R. 1986. *Coastal and Estuarine Sediment Dynamics*, Wiley, New York.

Feng, J., Mehta, A. J., Williams, D. J. A., and Williams, P. R. 1992. "Laboratory Experiments on Cohesive Soil Bed Fluidization by Water Waves," Report UFL/COEL-92/015, University of Florida, Gainesville.

Gade, H. G. 1958. "Effects of Non-rigid, Impermeable Bottom on Plane Surface Waves in Shallow Water," *Journal of Marine Research*, Vol 16, No. 2, pp 61-82.

Jiang, F. 1993. "Bottom Mud Transport Due to Water Waves," Ph.D. dissertation, University of Florida, Gainesville.

Jiang, F., and Mehta, A. J. 1992. "Some Observations on Fluid Mud Response to Water Waves," *Dynamics and Exchanges in Estuaries and the Coastal Zone*, D. Prandle, ed., American Geophysical Union, Washington, DC, pp 351-376.

Mathew, J. 1992. "Wave-Mud Interaction in Mudbanks," Ph.D. dissertation, Cochin University of Science and Technology, Cochin, Kerala, India.

McLellan, T. N., Pope, M. K., and Burke, C. E. 1990. "Benefits of Nearshore Placement," *Proceedings, Third Annual Technical Conference*, Florida Shore and Beach Preservation Association, Tallahassee, FL, pp 339-353.

Migniot, C. 1968. "Étude des Propriétés Physiques de Différents Sédiments tres fins et de leur Comportement sous des Actions Hydrodynamiques," *La Houille Blanche*, No. 7, pp 591-620.

Nair, A. S. K. 1988. "Mudbanks (Chakara) of Kerala—A Marine Environment to Be Protected," *Proceedings, National Seminar on Environmental Issues*, Golden Jubilee Seminar, University of Kerala, India, pp 76-93.

Teeter, A. M. 1992. "The Viscous Characteristics of Channel-Bottom Muds," *Dredging Research Technical Notes* DRP-2-04, U.S. Army Engineer Waterways Experiment Station, Vicksburg, MS.

Wells, J. T. 1983. "Dynamics of Coastal Fluid Muds in Low-, Moderate-, and High-tide-range Environments," *Canadian Journal of Fisheries and Aquatic Science*, Vol 40, No. 1, pp 130-142.

Wells, J. T., and Kemp, G. P. 1986. "Interaction of Surface Waves and Cohesive Sediments: Field Observations and Geologic Significance," *Estuarine Cohesive Sediment Dynamics*, A. J. Mehta, ed., Springer-Verlag, New York, pp 43-65.